Available online at www.sciencedirect.com

Journal of Solid State Chemistry 177 (2004) 1939–1943

JOURNAL OF SOLID STATE CHEMISTRY

http://elsevier.com/locate/jssc

A new high-pressure phase of $LiAlO_2$

Xijun Li,[a] Takamichi Kobayashi,[a] Fuxiang Zhang,[b] Koji Kimoto,[a] and Toshimori Sekine[a],*

[a] *Advanced Material Laboratory, National Institute for Materials Science, 1-1 Namiki, Tsukuba, Ibaraki 305-0044, Japan*
[b] *Max-Planck Institute for Solid State Research, Heisenberstr. 1, 70569 Stuttgart, Germany*

Received 8 April 2003; received in revised form 15 September 2003; accepted 8 December 2003

Abstract

A new high-pressure phase of $LiAlO_2$ has been recovered through a shock recovery technique at pressures above 9 GPa. This new phase has been refined as a tetragonal structure with lattice parameters of $a = 0.38866(8)$ nm and $c = 0.83001(18)$ nm. Its calculated density is 3.51 g/cm^3, about 34% denser than γ-$LiAlO_2$. The aluminum and lithium cations in this new phase are six-fold coordinated, as in α-$LiAlO_2$ and the structure of this new phase is similar to tetragonal $LiFeO_2$. This new high-pressure phase is stable at temperatures up to 773 K.

1. Introduction

High-pressure technology is an important technique used to synthesize new dense materials. It enables us to produce a solid phase that is denser than the starting material. Although there are various high-pressure techniques, shock wave compression demonstrates a useful method to produce dense materials from their low-pressure phases. Examples include diamond from graphite [1], fullerites [2] and fullerene [3], super-hard cubic boron nitride from rhombohedral BN [4], cubic silicon nitride [5] and germanium nitride [6].

We have applied shock compression techniques to investigate the high-pressure phase transition in $LiAlO_2$. This type of lithium compound has potential applications in the energy industry as lithium battery cathodes [7]. $LiAlO_2$ has four known polymorphisms. The γ-phase has a tetragonal symmetry with the space group $P4_12_12$ [8] and a density of 2.615 g/cm^3. The orthorhombic β-phase has the same coordinated Li and Al cations as the γ-phase. The other two polymorphs can be synthesized from γ-phase under high pressures. One is the hexagonal α-phase with $NaHF_2$ structure synthesized at 3.5 GPa and 850°C [9]. Its density is 3.401 g/cm^3. The other is a monoclinic phase synthesized at an intermediate pressure and temperature [10]. Sorting by coordination number, all the cations in the α-phase are coordinated by six oxygen anions and those in the γ-phase by four oxygen anions. Lithium cations are six-fold coordinated and aluminum cations display both four- and six-fold coordination in the monoclinic phase. Experiments on $LiAlO_2$ at high pressures above 3.5 GPa have not been performed. It is expected that new dense high-pressure phases of $LiAlO_2$ may be stabilized at higher pressures.

In the present study, impact technology has been applied to compress γ-$LiAlO_2$ at pressures up to 48 GPa. We have succeeded in recovering a tetragonal, high-pressure phase of $LiAlO_2$ with all cations six-fold coordinated by oxygen. This new phase has a distorted NaCl structure similar to the tetragonal $LiFeO_2$ phase. It is denser than the α-phase.

2. Experiments

γ-$LiAlO_2$ powder with a purity higher than 99% was used in this study. The powder was used as received, and a mixture of γ-$LiAlO_2$ and copper powder (90 wt%) was used as the starting material. The starting materials were packed into steel containers. A propellant gun was used to accelerate a plastic projectile with a flyer plate (steel, aluminum or copper) to impact the container at the desired velocity. When the shock wave first enters the sample, a first shock condition of high pressure (P_{Hi})

---

*Corresponding author. Fax: +81-29-851-2768.
E-mail address: sekine.toshimori@nims.go.jp (T. Sekine).

0022-4596/$ - see front matter © 2004 Elsevier Inc. All rights reserved.
doi:10.1016/j.jssc.2003.12.014

and high temperature (T_{Hi}) is simultaneously generated. This shock condition reaches the equilibrium pressure (P_{Hf}) and temperature (T_{Hf}) after the shock wave has been reflected several times within the sample. This reflectance is due to the difference between the shock impedance of the sample and that of the container material. The recovered container was then mechanically cut open. Nitric acid solution was used to remove copper if a mixture was used as the starting material. Details of the recovery experiments can be found in Ref. [11]. Post-shock samples as well as the starting material were investigated by X-ray diffraction (XRD) using Cu$K\alpha$ radiation, analytical electron microscopy (TEM), and electron energy loss spectroscopy (EELS).

3. Results and discussions

The shock conditions (P_{Hi}, T_{Hi}, P_{Hf} and T_{Hf}) are listed in Table 1 with other physical properties of the starting materials. The pressures, P_{Hi} and P_{Hf}, and their corresponding temperatures for mixtures of $LiAlO_2$ and copper were calculated with the shock impedance matching method [12] based on Hugoniot data [13] and thermodynamic constants of solid copper and porous copper. For shots on pure γ-$LiAlO_2$ powder, the shock temperatures and initial pressure were estimated based on thermal constants and Hugoniot data of sapphire. Sapphire was used for the estimate because of the lack of $LiAlO_2$ data. This approximation may produce a 10% and 20% uncertainty in P_{Hi} and T_{Hi} for shots on pure $LiAlO_2$ and 5% and 10% uncertainty in pressure and temperature for the mixed powder, respectively.

XRD patterns for all the recovered samples of all the runs together with the starting γ-$LiAlO_2$ are illustrated in Fig. 1, where the runs 848, 852, 950, and 955 are all for a Cu/γ-$LiAlO_2$ mixture (see Table 1). As can be seen in the figure, it appears that the intensities of some of the diffraction peaks decrease with increasing pressure and temperature while those of other peaks increase. The ones that increase correspond to the diffractions of a spinel type $Al_{2.5}Li_{0.5}O_4$ and its calculated lattice constant is 0.7914(2) nm (from run 895), which is consistent with its reported value [14]. The peaks that decrease indicate the presence of a new phase, and they have been indexed as a tetragonal structure. The structure refinement by FullProf. program has been carried out with the Rietveld method [15]. The observed and calculated d values of the new phase in the run 950 are compared in Table 2, with lattice parameters of $a = 0.38866(8)$ and $c = 0.83001(18)$ nm, four molecules of $LiAlO_2$, and its space group of $I4_1/amd$ (No. 141). The space group has been selected based on the known tetragonal $LiFeO_2$(18), and it is reasonable (Table 2). The density of this new phase is calculated to be 3.51 g/cm^3, about 34% denser than the γ-phase. The atomic arrangements in real space of this new phase and spinel $Al_{2.5}Li_{0.5}O_4$ are illustrated in Fig. 2. A comparison is given in Fig. 3 by taking into account the coexistence of the spinel phase. Table 3 summarizes the refined structural data for the new phase. The calculated atomic occupancy suggests some defects and disordering in the new phase. In spinel $Al_{2.5}Li_{0.5}O_4$, Li atoms are coordinated by six oxygen atoms and Al by both six

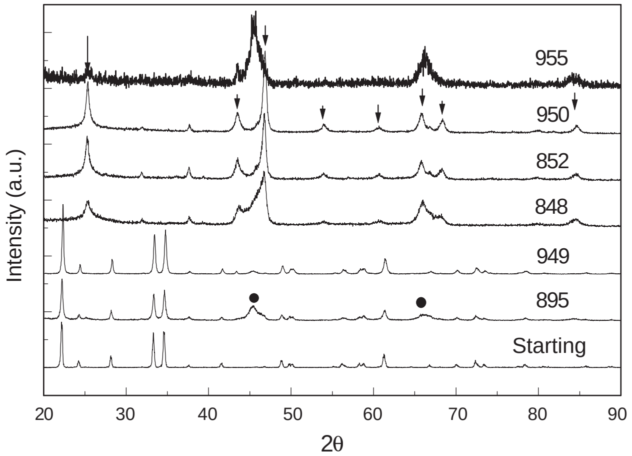

Fig. 1. XRD results for γ-$LiAlO_2$, and recovered samples 848, 852, 895, 949, 950 and 955. Samples 895 and 949 were obtained with pure γ-$LiAlO_2$ powder while the others were obtained from a mixture of γ-$LiAlO_2$ and copper. Peaks for the new phase δ-$LiAlO_2$ are marked by arrows; the dot-marked bands in sample 895 indicate the overlapped diffractions of Li_2O and spinel.

Table 1
List of shock conditions

Shot no.	Flyer material	Starting material	Impact velocity (km/s)	Sample density (g/cm^3)	Sample thickness (mm)	P_{Hi} (GPa)	T_{Hi} (K)	P_{Hf} (GPa)	T_{Hf} (K)
848	Steel	Mixture[a]	1.49	6.11	1.1	21	760	33	1100
852	Steel	Mixture[a]	1.07	6.50	1.8	15	600	22	780
895	Steel	$LiAlO_2$	1.51	1.92	1.2	7.5	<350	35	<700
949	Copper	$LiAlO_2$	2.00	2.24	0.5	10	<400	48	<900
950	Al	Mixture[a]	0.77	6.43	1.8	6.2	420	9	500
955	Steel	Mixture[a]	1.99	6.48	1.9	30	1030	48	1570

[a] Mixture of 10 wt% γ-$LiAlO_2$ and 90 wt% copper powder.

Table 2
X-ray diffraction data of a new phase δ-LiAlO$_2$

h	*k*	*l*	Observed *d* (nm)	Calculated *d* (nm)
1	0	1	0.35123	0.35191
0	0	4	0.20761	0.20765
2	0	0	0.19387	0.19424
2	1	1	0.16962	0.17006
1	0	5	0.15245	0.15275
2	0	4	0.14171	0.14186
2	2	0	0.13717	0.13735
2	1	5	0.12009	0.12007
2	2	4	0.11442	0.11456

This phase is indexed with a tetragonal symmetry with lattice constant $a = 0.38866(8)$ nm and $c = 0.83001(18)$ nm. The calculated density at room temperature is 3.51 g/cm^3 with $Z = 4$.

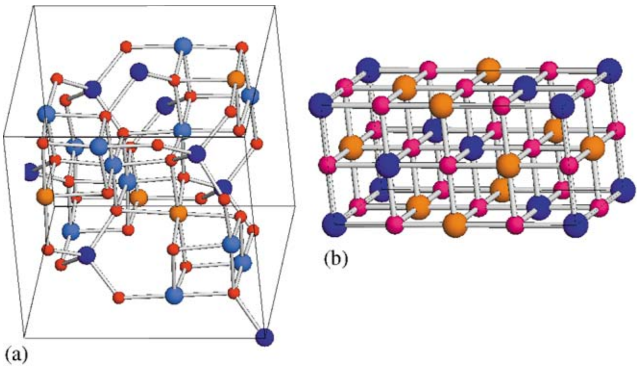

Fig. 2. Atom arrangements in spinel Al$_{2.5}$Li$_{0.5}$O$_4$ (a) and δ-LiAlO$_2$ (b). Oxygen, lithium, and aluminum atoms are illustrated by small (red), large (blue), and medium (yellow) spheres, respectively. It is obvious that all Li atoms in the spinel phase are six-fold coordinated, 40% of Al atoms are four-fold coordinated and 60% of Al atoms are six-fold coordinated (a) and both Li and Al are six-fold coordinated in δ-phase (b).

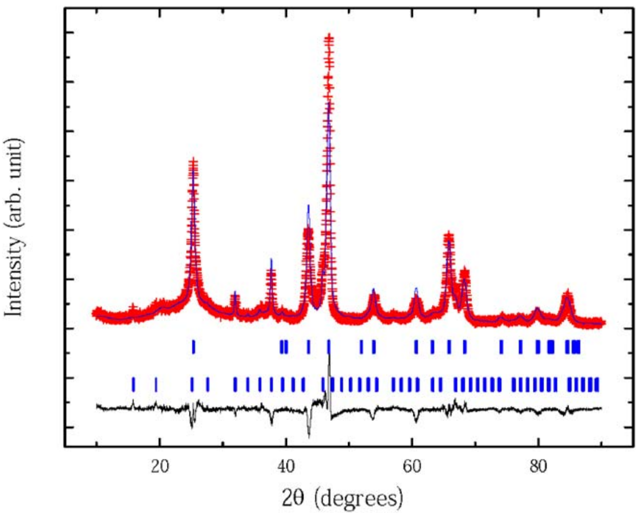

Fig. 3. A comparison of XRD patterns. Plus (+) is the observed one, the overwritten curve is the calculated pattern, and the bottom curve indicates the difference between the two. Two series of vertical bars mark the Bragg positions of new phase δ-LiAlO$_2$ and spinel Al$_{2.5}$Li$_{0.5}$O$_4$, respectively.

Table 3
Refined structural data for the new phase δ-LiAlO$_2$ with conventional Rietveld *R*-factor of 12.9

Atom	Wickoff	*x*	*y*	*z*	*B*	Occ.
Li	4*b*	0	0.75	0.625	2.19	0.814(13)
Al(2)	4*b*	0	0.75	0.625	1.5	0.186(13)
Al	4*a*	0	0.75	0.125	1.5	0.826(26)
Li(2)	4*a*	0	0.75	0.125	2.19	0.174(26)
O	8*e*	0	0.75	0.34877(55)	1.00	1

Space group $I4_1/amd$ (No. 141), $a = 0.38866(8)$ and $c = 0.83001(18)$. Positions (x, y, and z), thermal parameter (B) of each atom, and site occupancy (occ.) are given together with their deviations.

and four oxygen atoms, while all Li and Al are six-fold coordinated by oxygen in the new phase.

To characterize the chemical composition of the new phase, analytical electron transmission microscopy and EELS have been applied to sample 848. EELS spectra of lithium and aluminum in the selected area have been obtained. Based on EELS spectra of lithium and aluminum, the atomic number ratio of Li/Al was 1 ± 0.1. According to the EELS data, the selected material should be LiAlO$_2$, because Al$_{2.5}$Li$_{0.5}$O$_4$ has a Li/Al ratio of 0.2. The *K* edge absorption of Li in γ-LiAlO$_2$, the recovered sample and LiF (as a reference) are illustrated in Fig. 4(a). The *K* absorption edges ($\sim$62 eV) of the selected area and LiF are similar. This similarity shows that Li atoms in the new phase are six-fold coordinated. From Fig. 4(b), the similarity of the *L* absorption edge of aluminum in the new phase to that in α-Al$_2$O$_3$ indicates that Al is six-coordinated, while the Al-*L* edge absorption of γ-LiAlO$_2$ indicates the presence of four-coordinated aluminum cations. The spectra for spinel type Al$_2$O$_3$ differ from those of γ-LiAlO$_2$ and α-Al$_2$O$_3$. In conclusion, EELS spectra indicate that both Li and Al are four-fold coordinated in γ-LiAlO$_2$. This result differs from a nuclear magnetic resonance (NMR) study on γ-LiAlO$_2$, where ^{7}Li was probed [16]. In that study lithium was found to be six-fold coordinated but according to the NMR shift of lithium oxide, shifts of ^{7}Li are less than 10 ppm (Ref. [17]). This finding seems to be beyond the resolution of Ref. [16]. Therefore, the results of Ketty et al. on coordination number for γ-LiAlO$_2$ may not be conclusive. The EELS data support the structure obtained by Marezio from single-crystal XRD data [8]. Furthermore our results clearly indicate that both Li and Al are coordinated by six oxygen atoms in the new phase. This result is consistent with the refined structure (Fig. 2b).

Based on the present XRD results and EELS spectra, a new high-pressure phase of LiAlO$_2$ was recovered. We call it δ-LiAlO$_2$. In order to obtain more information about the phase transition of γ-LiAlO$_2$ to δ-LiAlO$_2$ and

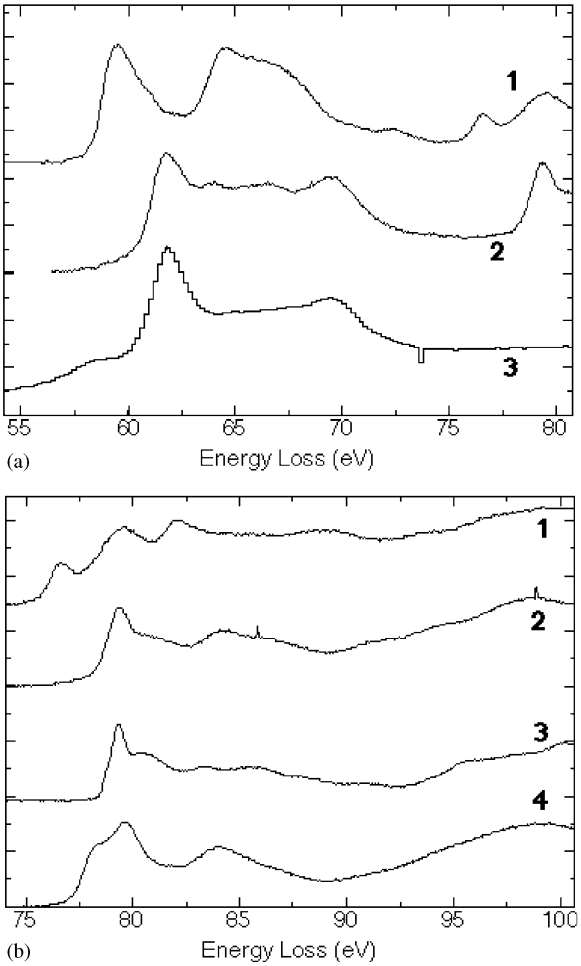

Fig. 4. (a) EELS spectra of Li-*K* in γ-$LiAlO_2$ (1), δ-$LiAlO_2$ (2) and LiF (3). (b) EELS spectra of Al-$L_{2,3}$ in γ-$LiAlO_2$ (1), δ-$LiAlO_2$ (2), α-Al_2O_3 (3), and γ-Al_2O_3 (4). XRD results for stability of δ-$LiAlO_2$ at high temperatures. Sample 950 with almost pure δ-$LiAlO_2$ was heated at 773, 843, 923 and 1073 K for 1 h, respectively, and the 923 K sample was further heated at 1173 K for 1 h.

phase stability of δ-$LiAlO_2$, shots done on pure γ-$LiAlO_2$ are depicted in Fig. 1 (runs 895 and 949). They are similar to the starting materials except for the addition of two broad diffraction lines, marked with dots in the figure. These broad bands correspond to the strongest diffractions of spinel $Al_{2.5}Li_{0.5}O_4$ and Li_2O. This can be explained as the following reaction:

$$5\,LiAlO_2 = 2\,Al_{2.5}Li_{0.5}O_4 + 2\,Li_2O.$$

Spinel $Al_{2.5}Li_{0.5}O_4$ can result from the decomposition of $LiAlO_2$, instead of transition to δ-$LiAlO_2$, under shock-induced high-temperature and high-pressure conditions, although the product Li_2O was removed during the treatment by nitric acid of samples 848, 852, 950 and 955. From Table 1, shots 895 and 949 have a very low initial shock pressures and low shock temperatures because pure γ-$LiAlO_2$ was used as a starting material, and these samples do not indicate the transition of γ- to δ-$LiAlO_2$. Copper powder can act as an efficient agent of both heating samples and enhancing pressures. The recovered powder 949 was observed to be only slightly sintered while sample 895 was well sintered, indicating that a higher temperature was generated in shot 895 than in shot 949. At enough high temperatures, $LiAlO_2$ was decomposed to spinel $Al_{2.5}Li_{0.5}O_4$. So spinel $Al_{2.5}Li_{0.5}O_4$ is a byproduct from high temperature decomposition of γ-$LiAlO_2$, while δ-$LiAlO_2$ will be a product of high-pressure solid–solid phase transition. Sample 955, which experienced the highest peak pressure of 48 GPa, is found to contain a certain amount of δ-phase (Fig. 1). This indicates that δ-$LiAlO_2$ is still stable at shock pressures up to 48 GPa.

It is worthy to address the structural similarity between $LiAlO_2$ and $LiFeO_2$. $LiFeO_2$ has three polymorphisms (with rhombohedral, cubic, and tetragonal symmetry, respectively) of NaCl or distorted NaCl structure, in which both Li and Fe are six-fold coordinated by oxygen. $LiAlO_2$ has five polymorphisms, a monoclinic phase, rhombohedral α-phase, orthorhombic β-phase, tetragonal γ- and δ-phases. In general, the radius of Al^{3+} ion in $LiAlO_2$ is close to that of Fe^{3+} in $LiFeO_2$. α-$LiAlO_2$ is isostructural to the rhombohedral $LiFeO_2$. According to solid-state chemistry [18], isostructurality can be expected between phases of $LiAlO_2$ and $LiFeO_2$, but the previously known tetragonal γ-$LiAlO_2$ does have a different structure to that of tetragonal $LiFeO_2$ as seen in different coordination enviroments of the cations. However, our obtained δ-$LiAlO_2$ appears to be isostructural to tetragonal $LiFeO_2$. The structural similarity between α-$LiAlO_2$ and rhombohedral $LiFeO_2$, and that between δ-$LiAlO_2$ and tetragonal $LiFeO_2$ indicates that high-pressure phases of $LiFeO_2$ can shed some light on the possible high-pressure structure of $LiAlO_2$, beyond the δ-phase. These possible candidates may have a CsCl type or distorted CsCl structure.

We have also investigated the temperature stability of δ-$LiAlO_2$. Several samples taken from sample 950, which consists of nearly pure δ-$LiAlO_2$, were heated in the atmosphere at 773, 843, 923, 1073 and 1173 K for 1 h, respectively. The XRD of each heated sample is shown in Fig. 5. δ-$LiAlO_2$ is stable up to 773 K. When heated to 843 K, a certain amount of α-phase was detected. With increasing temperatures up to 923 K, most of the δ-phase turned into α-phase. A little γ-phase appeared when the sample was heated to 1073 K. The sample heated at 1173 K produced the γ-phase. These heating experiments indicate a series of reversed transformations to the low-pressure phase with increasing temperature. The phase transitions of $LiAlO_2$ from δ- to α-phase and from α- to γ-phase reinforce that the composition of δ-phase has the same chemical composition as $LiAlO_2$. The phase-transition temperature from

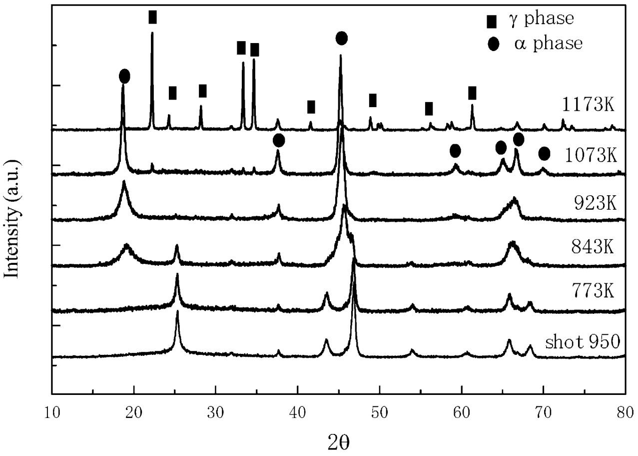

Fig. 5. XRD results for stability of δ-$LiAlO_2$ at high temperatures. Sample 950 with almost pure δ-$LiAlO_2$ was heated at 773, 843, 923, and 1073 K for 1 h, respectively, and the 923 K sample was further heated at 1173 K for 1 h. XRD measurements were performed at ambient conditions.

α- to γ-$LiAlO_2$ is about 1073 K, which is consistent with reported results [19].

It is interesting to examine the pressure ranges when α- and δ-phase are stable. According to the heating results mentioned above, it appears that δ-$LiAlO_2$ is a high-pressure stable phase compared to α-$LiAlO_2$. This is because an increase in temperature always tends to decrease the density of a solid while a rise in pressure increases it. However, when $LiFeO_2$ is considered, its temperature stability is different. $LiFeO_2$ with rhombohedral symmetry is a low-temperature phase while $LiAlO_2$ with tetragonal symmetry is the low-temperature case. Because the pressure ranges from 3 to 9 GPa is out of our experimental capability, we cannot get direct information on the possibility of synthesizing α-$LiAlO_2$ by shock compression. It may be useful to increase static high pressures applied to $LiAlO_2$ up to 10 GPa to investigate the possibility of synthesizing this new high-pressure phase. This technique is currently out of our research range.

It should be interesting to extend the same shock recovery experiments of $LiAlO_2$ to its analogue compounds, such as $LiBO_2$, $NaAlO_2$ and $LiGaO_2$. Several shock compressions on pure powders or powders mixed with copper have been conducted for each oxide mentioned above in the pressure ranges of 10–60 GPa and temperature ranges of 700–2500 K. No new phase was successfully detected by the XRD investigation on the recoveries. Some attention should be paid to the following observations: (1) phase-structure similarity between $LiAlO_2$ and $LiGaO_2$ at pressures up to 3.5 GPa [10] may not be extrapolated to the higher-pressure range, and (2) a long-term diffusive process, not realized by shock compression, may play an important role in these compounds.

4. Conclusions

A new high-pressure phase of $LiAlO_2$ (δ-phase), in which both lithium and aluminum are six-fold coordinated, has been synthesized from shock compressed γ-$LiAlO_2$. It is denser than α-phase. This new δ-phase is stable when shocked to 48 GPa at 1600 K. It is also stable when heated in the atmosphere at 773 K. δ-$LiAlO_2$ is isostructural to tetragonal $LiFeO_2$, while an isostructure to rhombohedral $LiFeO_2$ is α-$LiAlO_2$.

Acknowledgments

Xijun Li thanks the Japan Society for the Promotion of Science (JSPS) for his stay in NIMS.

References

[1] N. Setaka, Y.J. Sekikawa, J. Mater. Sci. 16 (1981) 1728–1730.
[2] T. Sekine, Proc. Jpn. Acad. B: Phys. 68 (1992) 95–99.
[3] H. Hirai, K.I. Kondo, T. Ohwada, Carbon 31 (1993) 1095–1098.
[4] T. Sekine, T. Sato, J. Appl. Phys. 74 (1993) 2440–2444.
[5] T. Sekine, H. He, T. Kobayashi, M. Zhang, F. Xu, Appl. Phys. Lett. 76 (2000) 3706–3708.
[6] H. He, T. Sekine, T. Kobayashi, K. Kimoto, J. Appl. Phys. 90 (2001) 4403–4406.
[7] G. Ceder, Y.M. Chiang, D.R. Sadoway, M.K. Aydinol, Y.I. Jang, B. Huang, Nature 392 (1998) 694–696.
[8] M. Marezio, Acta Crystallogr. 19 (1965) 396–400;
M. Marezio, J.P. Remeika, J. Chem. Phys. 44 (1966) 3143–3144.
[9] H.A. Lehmann, H.Z. Hesselbarth, Z. Anorg. Allg. Chem. 313 (1961) 117–120.
[10] C.H. Chang, J.L. Margrave, J. Am. Chem. Soc. 44 (1968) 2020–2022.
[11] T. Sekine, Eur. J. Solid Inorg. Chem. 34 (1997) 823–833.
[12] M.H. Rice, R.G. McQueen, J.M. Walsh, in: Solid Sate Physics, Vol. 3, Academic Press Inc., New York, 1958, p. 1.
[13] S.P. Marsh (Ed.) in: LASL Shock Hugonit Data, University of California Press, Berkeley, 1980.
[14] R. Farmeri, F. Queyroux, J. Gilles, J. Solid State Chem. 30 (1979) 257–263.
[15] D. Louer, M. Louer, J. Appl. Crystallogr. 5 (1972) 271–275;
A. Boultif, D. Louer, J. Appl. Crystallogr. 24 (1971) 987–993;
H.M. Rietveld, J. Appl. Crystallogr. 2 (1969) 65–71.
[16] T.R.T. Kutty, M. Nayak, Mater. Res. Bull. 34 (1999) 249–262.
[17] Z. Xu, J.F. Stebbins, Nature 270 (1995) 1332–1334.
[18] W.G. Wycoff, in: Crystal Structures, 2nd Edition, Interscience Publishers, New York, 1967, 302pp.
[19] R.A. Ribeiro, G.G. Silva, N.D.S. Mohallem, J. Phys. Chem. Solids 62 (2001) 857–864.